Laser interferometry for future satellite gravimetry missions

Sheard B., Dehne M., Mahrdt C., Gerberding O., Müller V., Heinzel G. and Danzmann K.
Albert Einstein Institute Hannover and Centre for Quantum Engineering and Space-Time Research (QUEST),
Callinstraße 38, 30167 Hannover, Germany

Abstract
This report presents an overview of the status of the ongoing research and development of laser interferometry for future satellite gravimetry missions at the Albert-Einstein-Institute in Hannover, Germany.

Introduction

Laser interferometry has been suggested as a way to improve the ranging performance of future gravity field missions based on satellite-to-satellite tracking. There is much overlap with the developments on laser interferometry for monitoring inter-satellite distance fluctuations for the future space-based gravitational wave detector, Laser Interferometer Space Antenna (LISA). For further information about LISA see e.g. [REF1] and [REF2]. We have initially focused our analysis on inter-satellite ranging in a GRACE like configuration using a laser interferometer, although laser interferometer could conceivably be applied to gradiometry by using an optical readout of test masses (based on the technology developed for LISA Pathfinder [REF3]).

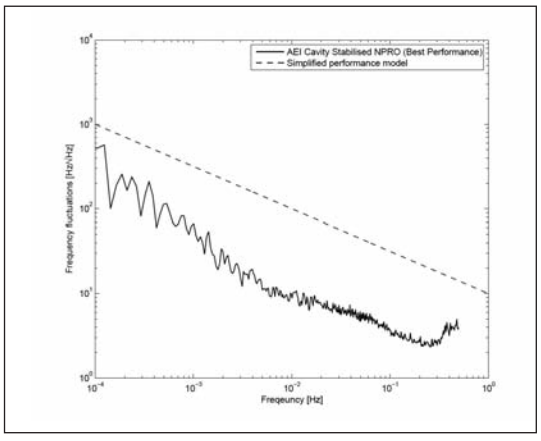

Figure 1: Differential laser frequency noise for two lasers each stabilised to a reference cavity in a separate vacuum chamber and a simplified performance model with margin [REF4].

Interferometer and system design aspects

For an inter-satellite ranging configuration like GRACE one of the major limiting noise sources is laser frequency noise due to the large inter-satellite distance (few hundred kilometres). Frequency noise couples into the inter-satellite range measurement according to the following relationship:

$$x_{\nu}(f) = \left(\frac{\lambda L}{c}\right)\nu(f)$$

where L is the spacecraft separation, c is the speed of light, λ is the operating wavelength (here assumed to be 1064 nm) and $\nu(f)$ is the amplitude spectral density of the laser frequency fluctuations. Thus the coupling of laser frequency noise scales linearly with the inter-spacecraft distance. The performance characteristics of a space qualified frequency stabilisation system are not yet known, however estimates from laboratory level experiments can be made. Figure 1 shows the differential laser frequency noise for two lasers each stabilised to a reference cavity in a separate vacuum chamber measured at the AEI and also a simplified performance model with margin.

Another significant consideration for inter-satellite interferometry is the Doppler shift due to

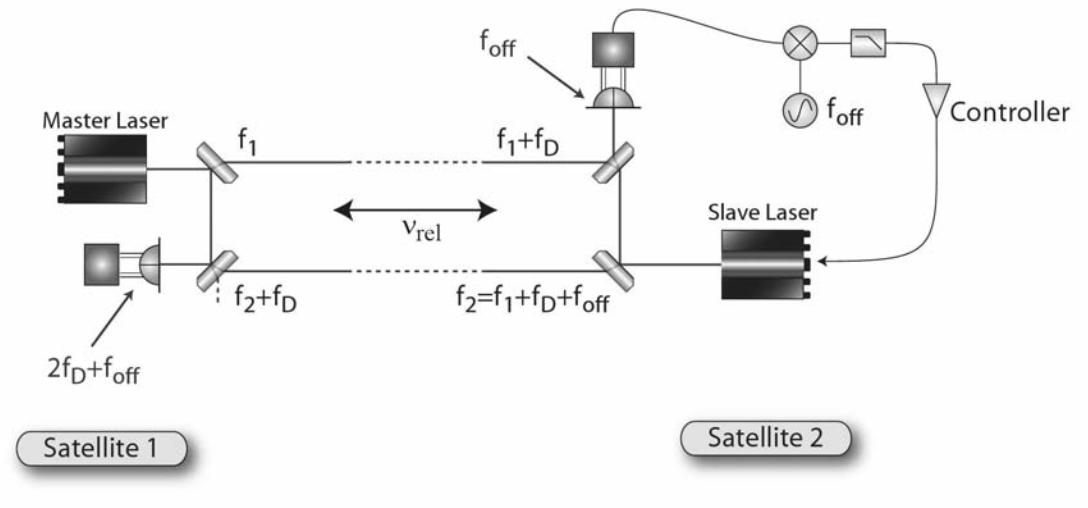

Figure 2: Offset phase locking in the presence of Doppler shifts. The transmit and receive paths are separated for clarity only. In reality the transmit and receive paths are collinear.

the relative velocity along the line-of-sight between the satellites. Figure 2 shows the frequencies measured by the photodetectors on each spacecraft in the presence of Doppler shifts due to the relative velocity along the line-of-sight. The one-way Doppler shift is given by

$$f_D = \frac{-v_{rel}}{\lambda}$$

where v_{rel} is the relative velocity along the line of sight and λ is the wavelength (1064 nm for the NPRO Nd:YAG lasers that will be used in LISA Pathfinder and LISA). The Doppler shift is larger for laser based interferometric ranging than that of a microwave ranging system, due to the smaller wavelength used. The measured beatnotes on both photodetectors must be within the phasemeter limits, which leads to the following constraints on the frequency offset used in the transponder and Doppler shifts:

$$f_{\min} \le f_{\text{off}} + 2f_D \le f_{\max}$$
$$f_{\min} \le f_{\text{off}} \le f_{\max}$$

where f_{min} and f_{max} is the minimum and maximum frequency respectively that the phasemeter can measure. Thus the phase measurement bandwidth places a constraint on the allowable relative spacecraft velocity along the line-of-sight and therefore is an important consideration when designing orbits of future satellite-to-satellite ranging systems, e.g. pendulum orbits. The current photodetectors and phasemeters prototypes for LISA have a bandwidth from 1 MHz to 20 MHz.

If a fixed offset with the optimal value of 10.5 MHz were used the allowable one-way Doppler shift is ±4.75 MHz (which is equivalent to a relative line-of-sight velocity of ±5 m/s for 1064 nm). The time evolution of the heterodyne frequency on each photodetector for this case is shown in figure 3. If it possible to roughly predict the Doppler shift (which is dominated by a sinusoidal component for a pendulum configuration) in real-time on-board each spacecraft, then by regularly adjusting the transponder offset frequency the tolerable relative velocity can be doubled to ±10 m/s (as shown in figure 4). Development of a phasemeter prototype with twice the LISA bandwidth has begun at the Albert Einstein Institute Hannover, which would allow ±10 m/s without an offset adjustment or ±20 m/s with an offset adjustment.

Although not presented here a detailed analysis of the optical link power budget with imperfect beam pointing with currently available laser powers has been carried out, allowing sizing of the transmitted beam and receiving aperture parameters. Strategies for link acquisition are also currently under investigation.

Polarising components

A key component of proposed interferometer

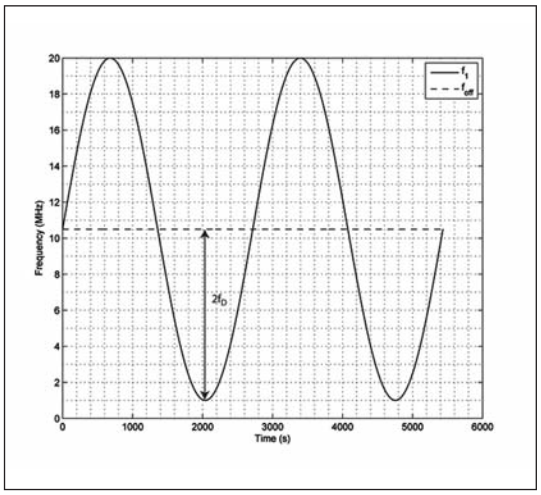

Figure 3: Heterodyne frequencies for constant offset

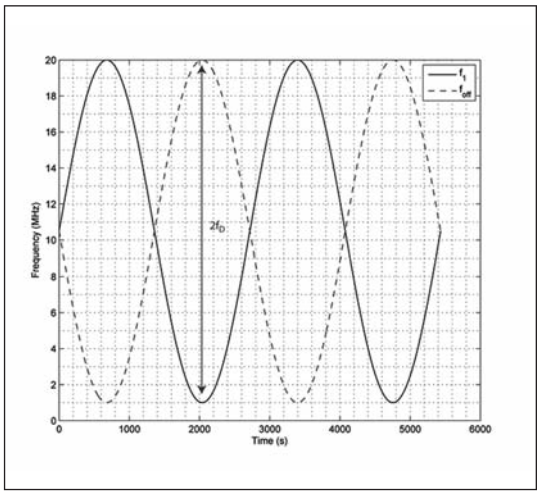

Figure 4: Heterodyne frequencies with variable offset

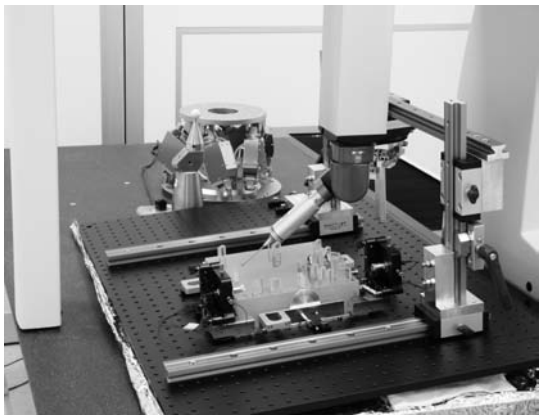

Figure 5: To place the components onto the optical bench a coordinate measuring machine in combination with an alignment tool was used.

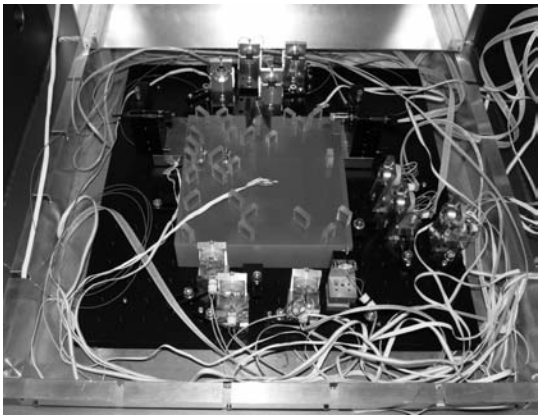

Figure 6: Implementation of the quasi-monolithic optical bench in the measurement environment.

designs are polarising optics. In order to investigate the influence of polarising components on interferometer sensitivity, an optical bench containing four different interferometers has been designed [REF5]. Two interferometers measure the position fluctuations of the same mirror (acting as test mass), but only one includes polarising optics. The remaining two interferometers are used for reducing noise, such as an active frequency stabilisation.

The hydroxide-catalysis bonding technique [REF6] was used to build the optical bench on an ultra-stable glass-ceramic baseplate made of Clearceram to compare polarising and non-polarising optics. For aligning the position of each optical component onto the optical bench a coordinate measuring machine in combination with an alignment tool was used. With the alignment setup depicted in figure 5 we achieved a positioning accuracy of the order of 10 µm.

In order to reduce coupling of acoustic and thermal effects into the phase readout the measurement was conducted in a vacuum chamber. For a further reduction of thermal noise, the optical bench was additionally enclosed by a thermal shield. Tests performed using the quasi-monolithic optical bench demonstrated a length stability orders of magnitude below the required stability for a straw-man design of future geodesy missions. The obtained noise performance is shown in figure 7.

That pre-experiment has validated that heterodyne interferometry using polarising optics is possible and that even picometre stability is

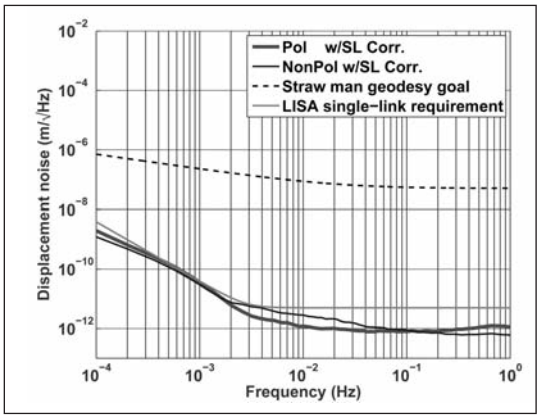

Figure 7: Noise performance of the polarising and non-polarising interferometer. A normalised stray-light correction is implemented in data post-processing. For comparison the LISA single-link requirement and a straw-man geodesy mission sensitivity goal are also shown.

achievable. Different stabilisations such as an amplitude stabilisation (DC laser intensity) and a stabilisation of the laser frequency are not yet implemented, so that we are confident that we are able to improve the sensitivity of the setup. Further breadboards to verify other interferometer concepts are under development.

Interferometer Simulations

All inter-satellite interferometers require analysis of propagation of non-Gaussian beams as from a practical point of view the received beam has to be clipped at the receiving aperture. The propagation of the non-Gaussian beam and the calculation of the interferometer signals have to be done by computer simulations. A software tool based on decomposition into Hermite-Gauss modes is under development and is currently under-going verification and validation.

Appropriate simulation tools to aid the design of the interferometer setup are needed because the conditions under which the final instrument will take data are not completely reproducible in laboratory experiments, for example effects related to the large spacecraft separation of approximately 200 km. Also the coupling of rotations of the satellites into the length measurement can be estimated and different interferometer topologies can be tested to optimise the layout and minimise the coupling.

The laser beam transmitted by the far spacecraft has to be clipped at the receiving telescope as it is not practical to build telescopes large enough to collect all of the light at the receiving telescope. Furthermore, large receiving apertures correspond to small receiving field-of-view as the heterodyne efficiency is inversely proportional to the receiving aperture radius. In practice one always has to clip the incoming light field at the receiving aperture and change its characteristic to a non-Gaussian field distribution. In order to simulate the propagation of non-Gaussian beams, numerical simulations have to be used since only few simple examples are analytically solvable.

Despite methods based on integration of diffraction integrals that are numerically challenging, the non-Gaussian light beam can be approximated by a set of higher order Hermite-Gauss modes which comprise a complete orthonormal set of functions. To approximate the non-Gaussian field distribution by Hermite-Gaussian modes, a unique amplitude for each mode is calculated via a two dimensional integral over the aperture plane [REF7]. To reconstruct the approximated field the modes are summed up weighted by the computed amplitudes. The calculation of the amplitudes and reconstruction of the field for signal calculation are the parts of highest computational cost. The propagation of the complete set can then be done by simple transformations of a complex parameter. Figure 8 shows the intensity distribution of an approximated top-hat beam up to order N=25 of considered Hermite-Gauss modes. The approximation considerably gains in accuracy if higher order mode components are included.

Since only a finite number of modes can be considered in the approximation, systematic errors in the calculated interferometer signals may occur.

Tests carried out for verification contain estimation of the error in the reconstructed field compared to the original distribution, comparison of propagated light fields generated by the mode expansion method and numerical integration. Also interferometer signals for appro-

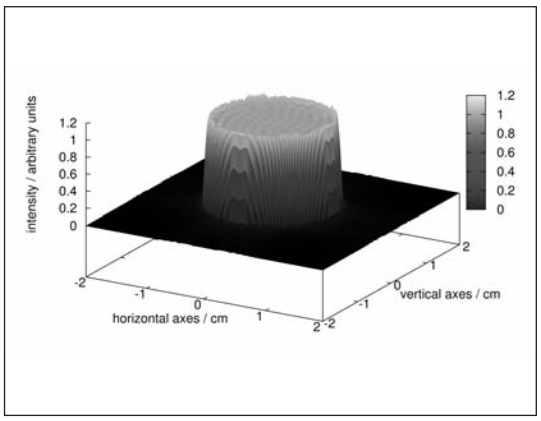

Figure 8: Intensity distribution of an approximated top-hat beam. The order of the highest included mode is 25.

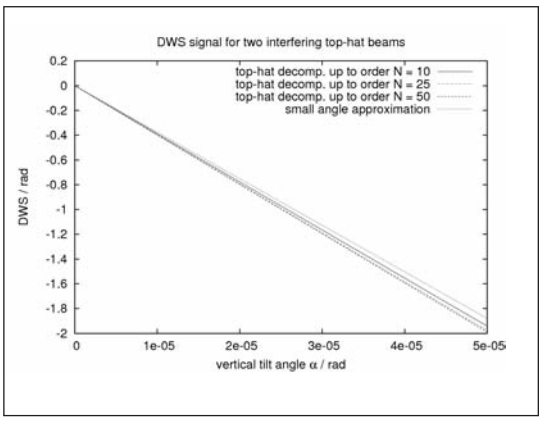

Figure 9: DWS signal for two interfering top-hat beams, comparing different orders of approximation and an approximate analytical result.

ximated fields were calculated and compared to known analytical results. Figure 9 shows the calculated differential wavefront sensing (DWS) signal for two interfering top-hat beams. The signal is shown for three different orders of approximation with the highest mode number being 10, 25 and 50 respectively and an approximate analytical result. The behaviour for small tilts is in good agreement with an approximate analytic result.

Future work will include optimisation of the algorithms for decomposition into Hermite-Gauss modes and the signal calculation by parallelisation and faster algorithms. Also simulation of interferometric setups for future geodesy missions will start.

Phasemeter

The readout of an inter-satellite interferometer is performed by a phasemeter, which measures the phase of the heterodyne beatnote between the incoming and local laser beam using a photodetector. The phasemeter consists mainly of an analogue front-end with anti-aliasing filters, analogue to digital converters and a FPGA, which contains the digital phasemeter core.

Relative satellite movements introduce Doppler shifts on the order of several MHz. The bandwidth of the phasemeter therefore constrains the relative inter-satellite velocity and possible orbit configurations. To address this problem, a phasemeter with a clock speed of 100MHz and a resulting bandwidth of 1 to 40 MHz was designed and tested, potentially doubling the allowable spacecraft relative velocity for a laser link compared to the previous designs. First results show that the phase-measurement performance is already better than that required for future geodesy missions.

After this proof of principle, a more detailed design of the analogue and digital components of the phasemeter needs to be carried out. Since the core of the phasemeter consists of a digital phase-locked-loop a linear digital model was created and verified by loop simulations. This model allows designing the phasemeter architecture for various noise influences, the required performance and minimal resources. Further investigations have to deal with nonlinear behaviours of the phasemeter and effects like cycle slipping. These studies will partly be performed by simulations and analytical methods. A signal generator, creating electrical input signals based on orbit and noise models, is under design, will be built and used to determine the actual phasemeter performance under realistic conditions.

An inter-satellite interferometer also allows measuring the alignment of the two satellites with very high precision. This technique is called differential-wavefront-sensing and is performed by a relative phase measurement of segments of a quadrant photodiode [REF9]. In future missions it will be used to measure the misalignment with very high precision and control the satellite attitude or beam steering

mechanism. The generation of this signal is also performed in the phasemeter. One potential readout scheme has already been designed and tested successfully in our prototype. Further investigations have to deal with offsets and noise sources in the analogue front-end of the phasemeter. A model for this readout is already included in our detailed digital model.
The phasemeter performs also the offset phase locking of the local laser to the received one. This control loop needs to be designed and tested. Analogue counterparts of this are already designed and in use.
Since the phasemeter is working at a clock speed of 100MHz, downsampling of the data has to be performed to a reasonable readout frequency, for example 10Hz. To reduce aliasing, a suitable filter has to be designed and tested. One possible filter design is used in the prototype and further designs are available, but remain to be validated. The connection of a microcontroller to the FPGA allows reducing the amount of filtering in the FPGA, to perform complicated DSP algorithms and include a higher level programming for intelligent operations. One possible candidate for this was evaluated and a new prototype including microcontroller is in development.
Another research field is the acquisition of the link between two satellites, which is a very complex and interesting problem. The phasemeters main task during this is the detection and acquisition of the beatnote signal between the local and remote lasers. Since the local laser frequency is controlled by the phasemeter, an intelligent algorithm needs to be designed to scan the degrees of freedom until lock is acquired. The microcontroller will allow developing an algorithm combining the different hardware levels. Such an algorithm can then be tried by applying electrical input signals similar to real mission conditions. The use of optical signals in different interferometer configurations will then be used to test the combination of the abilities mentioned before.

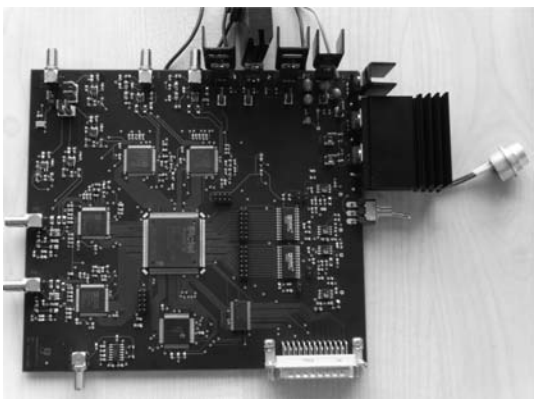

Figure 10: Phasemeter prototype

Orbit Simulator

An Orbit Simulation Toolkit (OSTK) for evaluating orbits and constellations for future gravity missions has been developed and tested. Models for Earth's static gravity field like the Earth Gravitational Model EGM08 are usually provided as coefficients of a spherical harmonic expansion. Various models have been implemented in OSTK to facilitate comparison between them. The time-variable components of the gravitational field can be expressed as time-dependent corrections of the spherical harmonic coefficients. The major contributions caused due to ocean tides (models: FES2004 & EOT 08a), atmospheric tides (Bode and Biancale) and solid Earth tides (IERS model) can be taken into account in the computations. Furthermore, the gravitational attraction due to other celestial bodies like Sun, Moon, Venus and Jupiter is non-negligible for precise orbit simulations. In OSTK planetary ephemeris data from JPL DE-405 catalogue is used to consider these perturbations.
Proper modeling of non-gravitational forces like drag and direct solar radiation pressure is sophisticated due to the dependency on environmental parameters as well as the satellites' attitude and surface properties. Presently simplified force models with fixed satellite attitude are used in the simulations. The atmosphere density is estimated using the empirical model NRLMSISE-00, which takes also the geomagnetic and solar activity into account. However, future development focuses on the implementation of 3D satellite models to allow an attitude dependent consideration of drag and solar radiation pressure.

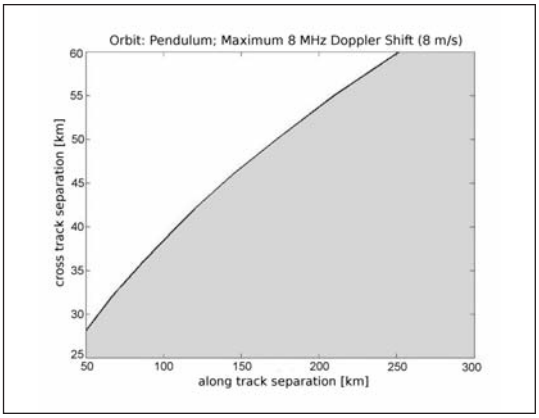

Figure 11: The grey area indicates orbits with Doppler shifts smaller 8 MHz

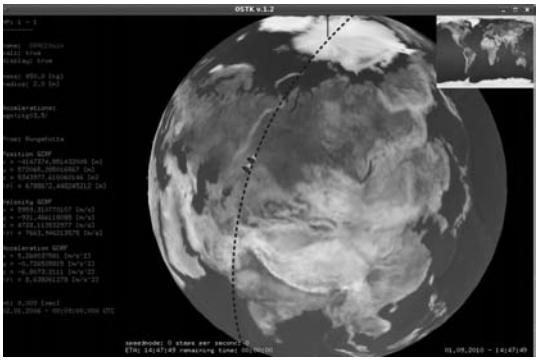

Figure 12: Screenshot of the graphical user interface of the OSTK

The orbit propagation itself is computed numerically by Runge-Kutta methods or an Adams-Bashforth-Moulton multistep procedure, though rough orbit estimations can be provided by Keplerian solutions.

The OSTK was used to simulate a satellite pair in pendulum orbit constellations with different cross-track separations, where the relative line-of-sight velocity served as a constraint. In figure 11 different pendulum orbit constellations at 480 km height and relative line-of-sight velocities of less than 8 m/s are shown as shaded area. Another future application can be found in the simulation of interferometer blinding periods by the Sun. Actual simulation results for a GRACE like constellation are being used to compare different approaches for processing GRACE Level-1b data [REF8]. Figure 12 shows the graphical user interface, which is used to configure and control the simulation scenarios as well as to provide visual feedback.

Acknowledgements

The Future Gravity Field Satellite Missions project is part of the R&D-Programme GEOTECHNOLOGIEN. This work was supported by the German Research Foundation (DFG) within the Cluster of Excellence QUEST (Centre for Quantum Engineering and Space-Time Research).

References

[REF1] K. Danzmann and A. Rüdiger, LISA technology—concept, status, prospects, Classical and Quantum Gravity 20, S1 (2003)

[REF2] D. A. Shaddock, Space-based gravitational wave detection with LISA, Classical and Quantum Gravity 25, 114012 (2008)

[REF3] P. McNamara, et al., LISA Pathfinder, Classical and Quantum Gravity 25, 114034 (2008).

[REF4] M. Troebs, Private Communication, 2007.

[REF5] M. Dehne et al., Laser interferometer for spaceborne mapping of Earth's gravity field, Journal of Physics: Conference Series 154, 012023 (2009)

[REF6] E. J. Elliffe et al., Hydroxide-catalysis bonding for stable optical systems for space, Classical and Quantum Gravity 22, S257-S267 (2005)

[REF7] Y. Liu and B. Lü, Truncated Hermite–Gauss series expansion and its application, Optik 117, 437–442 (2006)

[REF8] M. Naemi et al., Comparing Different Approaches for Processing GRACE Level-1 Data, EGU Gen. Ass., Vienna, Austria, 2010-05-02/0

[REF9] E. Morrison, et al., Automatic alignment of optical interferometers, Applied Optics 33, 5041-5049 (2004)